Estimation of Multiple Specific Growth Rates: Experimental Validation

Yves Pomerleau and Michel Perrier
Biotechnology Research Institute, National Research Council, Montréal, Canada, H4P 2R2

The experimental validation of on-line estimation of multiple specific growth rates for the bakers' yeast fed-batch process is presented. Pole placement based parameter estimation combined with an asymptotic biomass observer constitute the basic algorithm. The full process model being ill-conditioned for estimation using the available measured state variables, the use of two partial models related to two different states of the process is suggested. An alternating procedure between two sets of estimation algorithms designed from the partial models is proposed. The performance of the alternating procedure is validated both with simulated and experimental data. The accuracy of the estimates of the three specific growth rates involved in this process is verified according to two criteria based on the respiratory quotient and on the evaluation of the ethanol production/consumption rate.

Introduction

On-line estimation of the global specific growth rate in bioprocesses allows monitoring of the biological activity inside the fermentor. One possible approach is to consider the global specific growth rate as a time-varying parameter of a nonstationary system to be estimated on-line (Nihtila et al., 1984; Stephanopoulos and San, 1984; Dochain, 1986). If the global specific growth rate is divided in multiple components related to different catabolic pathways used by the micro-organism, the on-line estimation of these multiple specific growth rates gives a better insight of the biological activity in the fermentor.

In a previous article (Pomerleau and Perrier, 1990), theoretical developments of algorithms for on-line multiple specific growth rates estimation and biomass concentration estimation were presented. The algorithms were evaluated through simulation for the bakers' yeast fed-batch process in which three specific growth rates associated with the three primary catabolic pathways of the yeast have to be estimated. The performance of the algorithms was shown to be dependent on the choice of the measured state variables set: the performance was good for different sets except for one. Unfortunately, the worst case corresponds to the set of measured state variables easily available for this process which is composed of ethanol, dissolved oxygen and dissolved carbon dioxide concentrations. In this case, the yield coefficient matrix is poorly conditioned indicating a linear dependence of these three variables inside the yeast metabolism. The use of a partial model neglecting the ethanol consumption, with only two specific growth rates to be estimated, showed satisfactory results in the cases studied. However the use of this partial model alone did not allow the estimation of the three specific growth rates.

In this article, a procedure based on the alternate use of two sets of algorithms derived from two partial models is introduced and validated with experimental data. This procedure allows the on-line estimation of the three specific growth rates. The description of this procedure is presented in the first part of this article. It begins with a review of the process model and of the pole placement based specific growth rates estimation algorithm, including a biomass concentration observer. Then follows a description of the original concept of two partial models of the process and the presentation of the set of algorithms for each of them. Finally, the procedure of alternating use of these two sets of algorithms is introduced.

The second part of this article presents the experimental validation of this procedure. Special concerns have to be focused on the selection of the set of measured state variables for each partial model. Both mathematical and practical considerations are examined. The specific growth rates estimation results obtained during experimental fermentations with the best selection of measured state variables are then presented. Finally, two criteria based on the evaluated respiratory quotient

Correspondence concerning this article should be addressed to Y. Pomerleau.
M. Perrier is presently with the Pulp and Paper Research Institute of Canada.

and on the evaluated ethanol production/consumption rate are proposed to assess the validity of the estimates.

Process Model

The process model for the bakers' yeast fed-batch process has been already presented (Pomerleau and Perrier, 1990). The model is based only on mass balance equations over the liquid phase for biomass (x), substrate (s), ethanol (e), oxygen (c) and carbon dioxide (g). The resulting mass balance equations can be presented in the following matrix form:

$$\frac{d\xi}{dt} = -D*\xi + K*\varphi*x + U + M*x \tag{1}$$

where:

$\xi = [x\ s\ e\ c\ g]^T$ (state variable vector)

$\varphi = [\mu_o\ \mu_r\ \mu_e]^T$ (specific growth rate vector)

$U = [0\ D*s_i\ 0\ \text{OTR}\ \text{CTR}]^T$ (input/output vector)

$M = [0\ q_{s\text{man}}\ 0\ q_{o2\text{man}}\ q_{co2\text{man}}]^T$ (specific maintenance rate vector)

$$K = \begin{bmatrix} 1 & -\frac{1}{Y_o} & 0 & -\frac{1}{Y_{o2}} & \frac{1}{Y_{go}} \\ 1 & -\frac{1}{Y_r} & \frac{1}{Y_{re}} & 0 & \frac{1}{Y_{gr}} \\ 1 & 0 & -\frac{1}{Y_e} & -\frac{1}{Y_{o2e}} & \frac{1}{Y_{ge}} \end{bmatrix}^T$$ (yield coefficient matrix)

The presence of three specific growth rates reflects the capacity of the yeast to use different catabolic pathways. They are related to sugar oxidation (μ_o), sugar fermentation with ethanol production (μ_r) and ethanol oxidation (μ_e). No kinetic model for these specific growth rates is assumed. The ethanol output term is neglected and the input/output vector includes only the substrate feed ($D*s_i$), the oxygen transfer rate (OTR) and the carbon dioxide transfer rate (CTR). Specific maintenance uptake or production rates ($q_{s\text{man}}$, $q_{o2\text{man}}$ and $q_{co2\text{man}}$) have been included in the original model after that experimental results shown that up to 17% of the maximum oxygen uptake rate can be utilized for maintenance activity (Pomerleau, 1990).

Specific Growth Rates Estimation Algorithms

The process model can be partitioned in two subsets. The first subset includes the equations associated to the measured state variables (ξ_1), while the second subset is associated to the nonmeasured state variables (ξ_2):

$$\frac{d\xi_1}{dt} = -D*\xi_1 + K_1*\varphi*x + U_1 + M_1*x$$

$$\frac{d\xi_2}{dt} = -D*\xi_2 + K_2*\varphi*x + U_2 + M_2*x \tag{2}$$

For the estimation algorithm used, it is required that all input/output terms (U_1) in the measured state variable set are measured.

The specific growth rate estimation algorithm is derived from the measured state variable set only. First, a linear transformation is applied to the measured state variables set to decouple the equations in term of the specific growth rates:

$$\Psi = K_1^{-1}*\xi_1 \tag{3}$$

It is obvious that the number of measured state variables has to be at least equal to the number of specific growth rates to be estimated for the existence of the inverse or pseudo-inverse of K_1. An estimation algorithm based on pole placement (Pomerleau and Perrier, 1990) allows the estimation of the specific growth rates:

$$\hat{\Psi}_{t+1} = \hat{\Psi}_t + T*\left[-D_t*\Psi_t + \hat{\varphi}_t*x_t + K_1^{-1}*U_{1t} + K_1^{-1}*M_1*x_t + \frac{2*(1-p)*(\Psi_t - \hat{\Psi}_t)}{T} \right]$$

$$\hat{\varphi}_{t+1} = \hat{\varphi}_t + \frac{(1-p)^2*(\Psi_t - \hat{\Psi}_t)}{T*x_t} \tag{4}$$

This algorithm offers the advantage of providing a constant estimation error dynamics in spite of the nonlinearity of the process. The error dynamics is fixed by a single tuning parameter (p) which corresponds to a pole location in the discrete complex plane. The prediction equation (Ψ) has a closed loop term on the estimation error with a constant gain $[2*(1-p)]$. The adaption law (φ) is closely related to the generalized gradient method (Sastry and Bodson, 1989).

The nonmeasured biomass concentration appears in the equations of the estimation algorithm. A biomass concentration observer is thus needed for the application of the estimation algorithm. A reduced order observer (Narendra and Annaswamy, 1989), which takes benefit of the measured state variables to eliminate the specific growth rates from the observer equation (Dochain and Bastin, 1986), is designed. A transformed state variable is obtained by the linear transformation between measured state variables set and the biomass concentration:

$$Z = x - K_o*K_1^{-1}*\xi_1 \tag{5}$$

where K_o is a row vector with all elements equal to one.

The biomass concentration observer, in the discrete form, is then:

$$\hat{Z}_{t+1} = \hat{Z}_t + T*\left[(-D_t - K_o*K_1^{-1}*M_1)*\hat{Z}_t - K_o*K_1^{-1}*U_{1t} - K_o*K_1^{-1}*M_1*K_o*K_1^{-1}*\xi_{1t} \right] \tag{6}$$

The inclusion of maintenance terms in the process model adds two terms in the observer equation. The first term, $-K_oK_1^{-1}M_1Z_t$, has an influence on the stability and convergence properties of the observer. This term, being always negative for this process, shifts the pole of the observer dynamics

further left making the dynamics faster and insuring the stability even when the dilution rate is zero. The second term, $-K_o K_1^{-1} M_1 K_o K_1^{-1} \xi_{1t}$, has no influence on the observer performance because it is negligible in front of the input/output term, $-K_o K_1^{-1} U_{1t}$. The observed biomass concentration is obtained from the inverse transformation:

$$\hat{x}_t = \hat{Z}_t + K_o * K_1^{-1} * \xi_{1t} \tag{7}$$

This biomass concentration observer is independent of any kinetic expression for the specific growth rates.

As mentioned previously, the number of measured state variables has to be at least equal to the number of specific growth rates to be estimated. The application of this approach with the complete process model gives good results when the condition number of the yield coefficient matrix (K_1) of the measured state variable set (ξ_1) is low (Pomerleau and Perrier, 1990). Unfortunately, for the bakers' yeast process, the only set of three measured state variables available experimentally is composed of the ethanol, dissolved oxygen and dissolved carbon dioxide concentrations and the yield coefficient matrix is badly conditioned in this case. This poor conditioning of the yield coefficient matrix indicates a linear dependence of these three state variables inside the yeast metabolism. The determinant of this matrix would be null under the following condition:

$$\left(\frac{Y_{o2e}}{Y_{ge}} + \frac{Y_{re} * Y_{o2e}}{Y_e * Y_{gr}}\right) - \frac{Y_{o2}}{Y_{go}} = 0 \tag{8}$$

which is equivalent to:

$$RQ_f - RQ_o = 0 \tag{9}$$

The yield coefficient matrix is thus singular when the respiratory quotient (carbon dioxide produced over oxygen consumed) of the sugar oxidation pathway (RQ_o) is equal to the respiratory quotient associated with sugar fermentation followed by ethanol oxidation (RQ_f). In the present case, the two respiratory quotients are very close and the estimation of the three specific growth rates gives poor results with this set of three measured state variables. The use of partial process models overcomes this problem as explained below.

Partial Process Models

From a global point of view, the bakers' yeast fed-batch process can only be in an ethanol production state or in an ethanol consumption state. The process model can be divided in two partial models to represent these two states. The first partial model corresponds to the ethanol production state of the process and it is denoted as the respiro-fermentative partial model. The second partial model, the respirative partial model, corresponds to the oxidation state of the process where glucose and ethanol oxidation may occur. The matrix representation of the mass balance equations (Eq. 1) is still valid for both partial models. The difference between both models is reflected in the formulation of the specific growth rate vector (φ) and of the yield coefficient matrix (K). For the respiro-fermentative partial model, these two items are:

$$\varphi_{RF} = [\mu_o \quad \mu_r]^T$$

$$K_{RF} = \begin{bmatrix} 1 & -\frac{1}{Y_o} & 0 & -\frac{1}{Y_{o2}} & \frac{1}{Y_{go}} \\ 1 & -\frac{1}{Y_r} & \frac{1}{Y_{re}} & 0 & \frac{1}{Y_{gr}} \end{bmatrix}^T \tag{10}$$

and for the respirative partial model:

$$\varphi_R = [\mu_o \quad \mu_e]^T$$

$$K_R = \begin{bmatrix} 1 & -\frac{1}{Y_o} & 0 & -\frac{1}{Y_{o2}} & \frac{1}{Y_{go}} \\ 1 & 0 & -\frac{1}{Y_e} & -\frac{1}{Y_{o2e}} & \frac{1}{Y_{ge}} \end{bmatrix}^T \tag{11}$$

The application of the estimation algorithm to each partial model is straightforward. A complete set of biomass observer and specific growth rate estimator is designed for each partial model as presented in Table 1. As each of them contains only two specific growth rates, the set of measured state variables has to be composed of only two measured state variables. The problem of the linear dependence between ethanol, dissolved oxygen and dissolved carbon dioxide is thus avoided.

Using only one partial model algorithm set, the biomass and specific growth rate estimates converge when the process is in the corresponding state. But, when the state of the process does not correspond to the partial model used, the estimates diverge. According to the process time trajectory, the estimates

Table 1. Pole Placement Based Estimation Algorithms and Asymptotic State Biomass Observer for both Partial Process Models

Respiro-fermentative partial model Biomass observer:

$$\hat{Z}_{RF\,t+1} = \hat{Z}_{RF\,t} + T * [(-D_t - K_o * K_{1\,RF}^{-1} * M_{1\,RF}) * \hat{Z}_{RF\,t} - K_o * K_{1\,RF}^{-1} * U_{1\,RF\,t} - K_o * K_{1\,RF}^{-1} * M_{1\,RF} * K_o * K_{1\,RF}^{-1} * \xi_{1\,RF\,t}]$$

$$\hat{x}_{RF\,t} = \hat{Z}_{RF\,t} + K_o * K_{1\,RF}^{-1} * \xi_{1\,RF\,t}$$

Specific growth rates estimator:

$$\hat{\Psi}_{RF\,t+1} = \hat{\Psi}_{RF\,t} + T * [-D_t * \Psi_{RF\,t} + \hat{\varphi}_{RF\,t} * \hat{x}_t + K_{1\,RF}^{-1} * U_{1\,RF\,t} + K_{1\,RF}^{-1} * M_{1\,RF} * \hat{x}_t] + 2 * (1-p) * (\Psi_{RF\,t} - \hat{\Psi}_{RF\,t})$$

$$\hat{\varphi}_{RF\,t+1} = \hat{\varphi}_{RF\,t} + \frac{(1-p)^2 * (\Psi_{RF\,t} - \hat{\Psi}_{RF\,t})}{T * \hat{x}_t}$$

Respirative partial model Biomass observer:

$$\hat{Z}_{R\,t+1} = \hat{Z}_{Rt} + T * [(-D_t - K_o * K_{1\,R}^{-1} * M_{1R}) * \hat{Z}_{Rt} - K_o * K_{1\,R}^{-1} * U_{1\,Rt} - K_o * K_{1\,R}^{-1} * M_{1R} * K_o * K_{1\,R}^{-1} * \xi_{1\,Rt}]$$

$$\hat{x}_{Rt} = \hat{Z}_{Rt} + K_o * K_{1\,R}^{-1} * \xi_{1\,Rt}$$

Specific growth rates estimator:

$$\hat{\Psi}_{R\,t+1} = \hat{\Psi}_{Rt} + T * [-D_t * \Psi_{Rt} + \hat{\varphi}_{Rt} * \hat{x}_t + K_{1\,R}^{-1} * U_{1\,Rt} + K_{1\,R}^{-1} * M_{1R} * \hat{x}_t] + 2 * (1-p) * (\Psi_{Rt} - \hat{\Psi}_{Rt})$$

$$\hat{\varphi}_{R\,t+1} = \hat{\varphi}_R + \frac{(1-p)^2 * (\Psi_{Rt} - \hat{\Psi}_{Rt})}{T * \hat{x}_t}$$

provided by the use of only one partial model can or cannot be acceptable. In the case of the experimental fermentations presented in this article, the performance obtained with only one partial model is very poor (results not shown). The accumulated error on the observed biomass concentration due to process and model mismatch is too high and induces very poor estimated values of the specific growth rates.

In the same case with simulation data, it was found that the specific growth rate estimates converge rapidly to their real values when the process enters in the corresponding state if the actual instead of the observed biomass concentration was used. This suggests the possibility to use alternatively the sets of algorithms issued from both partial models so that the appropriate partial model is used according to the process state.

Alternating Procedure Using Both Partial Models

The procedure proposed is based on the use of the proper partial model algorithm set according to the process state. Two main problems have to be solved to obtain an efficient procedure:

- How to detect the transition between process states?
- How to make the transition between the two sets of algorithms?

The first problem is resolved by looking at the values of the specific growth rate estimates. When the process is not in the corresponding state, the specific growth rate estimate directly related to ethanol (μ_r in the respiro-fermentative model and μ_e in the respirative model) takes negative value. The criterion for the transition between partial model algorithm sets is given by the transition between positive and negative values of these estimates.

The transition procedure between the two sets of algorithms is a more complicated problem. If this is not done carefully, it introduces an important perturbation in the algorithms. In each algorithm set, five variables have to be monitored in time: the transformed variable estimate in the biomass observer (Z), the two transformed measured state estimates (Ψ) and the two specific growth rate estimates (φ). It is important to monitor the time course of these variables also when the algorithm set does not correspond to the process state to obtain appropriate values of these variables at transition time.

For the transformed variable in the biomass observer, the results show a strong divergence when the process is not in the state corresponding to the partial model. The time trajectory of this variable cannot be followed in this case because the estimation error will be too high when the process returns back in the corresponding state. To overcome this problem, the following technique is suggested. When the process state changes at time t, the transformed variable and the estimated biomass concentration at time $t-1$ issued from the other partial model algorithm set are used to provide an estimated value of the transformed variable of the new partial model at time $t-1$. Then the biomass observer algorithm of the new partial model is used. For example, consider the transition between respiro-fermentative model to respirative model at time t:

$$\hat{x}_{\mathrm{RF}\,t-1} = \hat{Z}_{\mathrm{RF}\,t-1} - K_o * K_{1\,\mathrm{RF}}^{-1} * \xi_{1\,\mathrm{RF}\,t-1}$$

$$\hat{Z}_{R\,t-1} = \hat{x}_{\mathrm{RF}\,t-1} + K_o * K_{1\,R}^{-1} * \xi_{1\,R\,t-1} \qquad (12)$$

For the specific growth rate estimates, distinct treatments are done depending if the specific growth rate is related or not to ethanol. In the case of the estimation of μ_o, the time trajectory is still followed during the period when the partial model algorithm set is not used. Experiences have shown that the estimation error is not so large and that convergence following the transition is so rapid that a more sophisticated treatment is not required. For ethanol related specific growth rates, μ_e or μ_r, the estimated value is forced to zero when the partial model does not correspond to the process state.

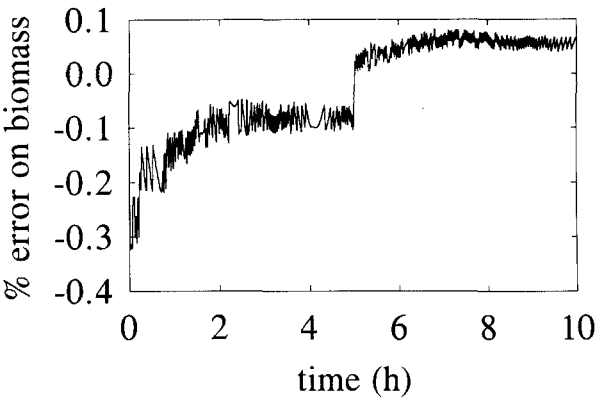

Figure 1. Percentage error on the observed biomass concentration obtained with simulation data.

For the transformed state variables of the specific growth rate estimator (Ψ), the time trajectories have also to be followed during partial model and process mismatch. But the estimated value for biomass concentration used during this period is the one issued from the valid partial model observer. Also, the zero value of the ethanol related specific growth rate estimate is used in the prediction equations. These two precautions with the closed-loop gain on these variables kept the predicted values near the real ones. This technique is required to avoid a too strong perturbation of the estimation algorithm at transition time.

This alternating procedure using two algorithm sets derived from the two partial models has been verified with simulation data. Figure 1 shows the error percentage between the estimated and the actual biomass concentrations. This percentage remains very low in spite of regular transitions between ethanol production and ethanol consumption state. The comparison between the estimated and real values of the three specific growth rates is shown in Figures 2, 3 and 4. These results are as good as the ones obtained with a full model based algorithm using a well conditioned measured state variable set (sugar, ethanol and dissolved oxygen for example, see Pomerleau and Perrier, 1990).

The quality of these results relies on the characteristic of the pole placement based estimation algorithm. The constant estimation dynamics of this algorithm can be fixed to a low time constant value so that the period between the process transition and the time which is detected by the estimation algorithm is reduced to a minimum value. This insures that the mismatch period between the process state and the partial model is kept very brief, whenever the process is dynamic.

Selection of the Measured State Variable Sets

Three measured state variables are available: ethanol, dis-

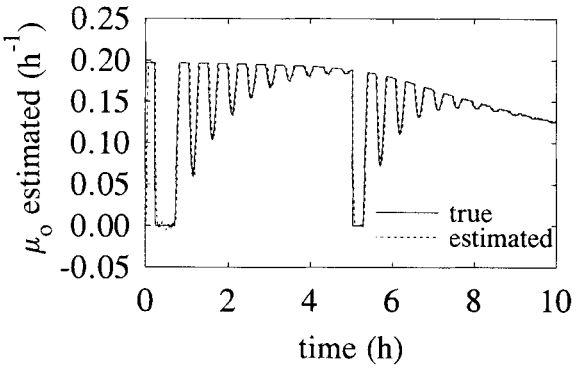

Figure 2. Actual and estimated sugar oxidation specific growth rate (simulation).

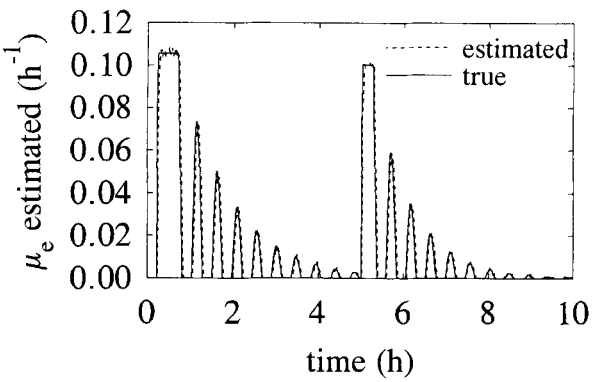

Figure 4. Actual and estimated ethanol oxidation specific growth rate (simulation).

solved oxygen, and carbon dioxide concentration. The use of the partial models alternating procedure requires only two measured state variables for each algorithm set. This allows the choice among nine possible combinations of measured state variables sets, three for each partial model algorithm set. The suggested procedure for selection of each measured state variable set is based on mathematical and practical considerations.

The mathematical considerations are the condition number of the yield coefficient matrix (K_1) of the measured state variable set and the value of the term associated to the maintenance ($K_o K_1^{-1} M_1$) present in the biomass observer. A high condition number causes a greater sensitivity of the estimates to the noise present in the measured signals and the maintenance term has an influence on the stability and convergence properties of the observer. Table 2 presents these two quantities for each measured state variable set and for each partial model. The condition number is in the same order of magnitude for all cases. The maintenance term is almost constant: in fact, its negative value insures the stability of the observer and provides a slightly faster convergence of the estimate.

The second consideration in the choice of the measured state variable set is the quality of each measured data signal. The ethanol concentration signal has a higher noise-to-signal ratio than the other measured data signals (dissolved oxygen and carbon dioxide concentrations, OTR and CTR). This fact combined with the absence of input/output term in the ethanol mass balance equation contributes to obtain noisier estimates of the specific growth rates when ethanol concentration is included in the measured state variable sets.

The selection of the dissolved oxygen and carbon dioxide concentrations in the measured state variables sets for both partial models should give the best performance.

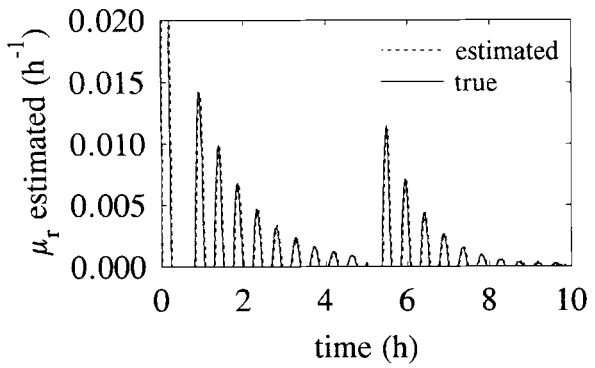

Figure 3. Actual and estimated sugar fermentation specific growth rate (simulation).

Experimental Verification

Experimental conditions

The experimental fermentations have been achieved in a 20 L BioEngineering fermentor. The yeast strain, *Saccharomyces cerevisiae*, was supplied by Lallemand Inc., an industrial bakers' yeast produced in Montreal. The carbon source was a mixture of cane and beat molasses also provided by the industrial producer. The operating conditions were chosen to reproduce the industrial fermentations.

The fermentations were carried out under ethanol concentration regulation with different nonlinear adaptive control laws (Pomerleau, 1990). The ethanol regulation keeps the process near the boundary between the ethanol production and ethanol consumption state. Set-point changes, agitation speed and aeration rate perturbations have been applied to test the control laws; Tables 3 and 4 give the description of these perturbations for the two fermentations presented. These perturbations create a diversity of process conditions and some of these can be considered as extreme conditions which do not appear in normal operation. The dissolved oxygen concentration was not controlled and the agitation speed (700 RPM) and the aeration rate [2 L/(L·min)] were kept constant except

Table 2. Condition Number of the Yield Coefficient Matrix (K_1) and Value of the Term $K_o K_1^{-1} M_1$ for both Partial Models and each Possible Set of Two Measured State Variables

Measured State Variables Set	*Condition Number of K_1*	*Value of $-K_O K_1^{-1} M_1$*
	Respirative Partial Model	
[e c]	11.8	−0.0300
[e g]	2.0	−0.0308
[e c]	4.4	−0.0306
	Respiro-Fermentative Partial Model	
[e c]	11.5	−0.0300
[e g]	15.1	−0.0308
[c g]	11.3	−0.0301

Table 3. Events for Fermentation 1

Time (min)	Events
0	Start of the Data Acquisition System
17	Start of the Closed-Loop Control
113	Change of Set-Point Value from 0.26 to 1.00 g/L
196	Change of Set-Point Value from 1.00 to 0.26 g/L
286	Decrease of Agitation Speed from 700 to 600 RPM
383	Increase of Agitation Speed from 600 to 700 RPM
494	Decrease of Airflow Rate from 16 to 13 L/min
541	Increase of Airflow Rate from 13 to 19 L/min
594	Stop of the Fermentation

at the time of perturbation. pH was kept constant at 5.0 where the variation of pH has no influence on the equilibrium of the different forms of dissolved carbon dioxide.

The ethanol concentration was measured in the exit gas with a Figaro sensor (TGS822) and calibrated as a function of the liquid ethanol concentration in the fermentor. Dissolved oxygen concentration was measured with an Ingold probe. Carbon dioxide concentration was presumed to be directly proportional to the carbon dioxide content of the exit gas. OTR and CTR were evaluated with off-gas analysis performed by a magnetic sector mass spectrometer (VG-MM8-80). The molasses feed rate was controlled by a variable speed peristaltic pump (Watson-Marlow 501U/R).

Results and Discussion

Figures 5, 6 and 7 show the time course of the different measured variables during fermentation 1. Ethanol set-point changes occur at time 17, 113 and 196 min and force the process to go in ethanol production or consumption state. This is also reflected in the value of the CTR which varies widely during these periods. The OTR increases until the 250th min and remains constant except during the perturbation period of the agitation speed or aeration rate. This constant OTR denotes that the fermentation was in oxygen transfer limitation confirmed by the nearly zero dissolved oxygen concentration.

Figure 8 shows the biomass concentration estimates produced by the alternating use of the two sets of algorithms issued from the two partial models. The comparison of this time profile with the measured biomass concentration values from different samples is also shown. The precision of the biomass concentration estimate is within the precision of the measured values. Note that this performance is not only linked to the biomass concentration observer characteristics but also

Table 4. Events for Fermentation 2

Time (min)	Events
0	Start of the Data Acquisition System
2	Start of the Closed-Loop Control
103	Transition from Nonadaptive to Adaptive Control Law
309	Return to Nonadaptive Control Law
399	Change of Set-Point Value from 0.25 to 0.16 g/L
457	Increase of Agitation Speed from 700 to 900 RPM
504	Transition from Nonadaptive to Adaptive Control Law
542	Stop of the Fermentation

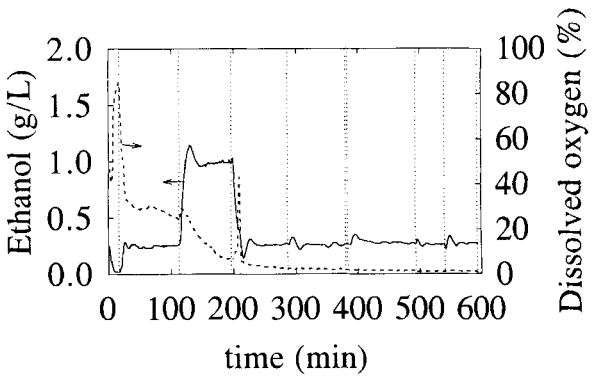

Figure 5. Ethanol and dissolved oxygen concentration in fermentation 1.

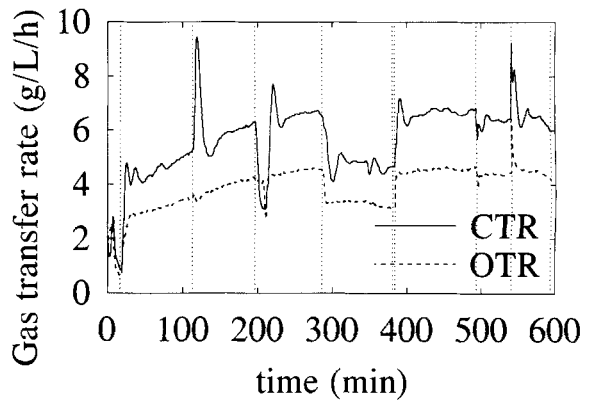

Figure 6. Oxygen and carbon dioxide transfer rate in fermentation 1.

on the ability of the specific growth rate estimator to detect the changes in the process state.

In Figure 9, the estimated values of specific growth rate associated with the sugar oxidation (μ_o) is shown with the specific oxygen transfer rate (SOTR) obtained from OTR divided by the estimated biomass concentration. The estimate of μ_o remains quite constant during the nonlimiting oxygen transfer condition and corresponds to the maximum specific growth rate achievable without ethanol production. In the

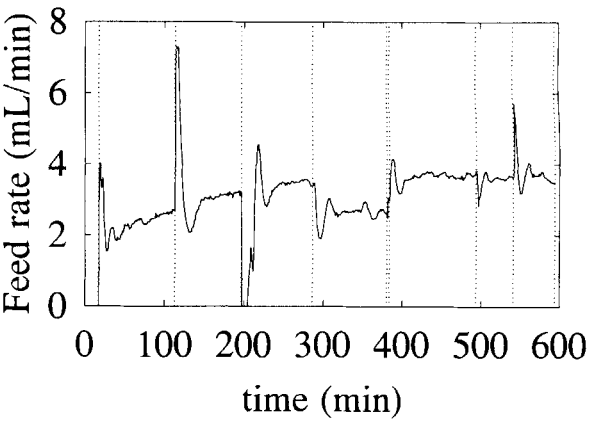

Figure 7. Substrate feed rate in fermentation 1.

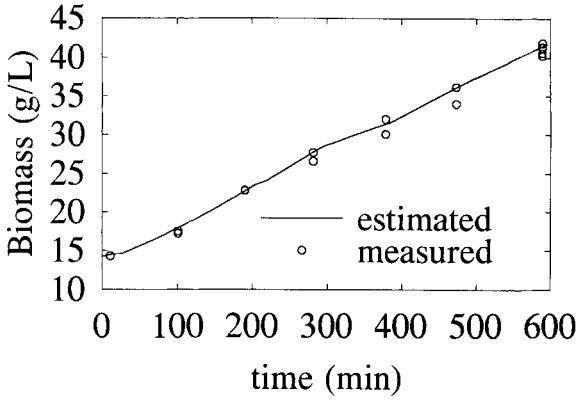

Figure 8. Estimated and measured biomass concentration in fermentation 1.

limiting oxygen transfer condition, this specific growth rate is reduced according to the decrease of the specific oxygen uptake rate.

The scales of this graph were adjusted such that the process is in ethanol production state when the μ_o estimate curve coincided to the SOTR one. In this case, the sugar uptake saturates the oxidation capacity of the yeast and the overflow of sugar is directed to the anaerobic pathway with ethanol production. When it is below, the sugar did not use all the oxidation capacity and allowed the ethanol oxidation. This is confirmed by the values of the estimates of the two other specific growth rates (μ_e and μ_r) presented in Figure 10. This behavior corresponds quite well with the hypothesis of the limiting oxidation capacity of the yeast (Sonnleitner and Kappeli, 1986).

The estimated values of the three specific growth rates show rapid fluctuations. Do these fluctuations correspond to process fluctuations or are they artifact of the overall estimation procedure? A first criterion to evaluate the accuracy of the three specific growth rate estimates is to compare the experimental and estimated respiratory quotient (RQ) obtained from the estimates of the three specific growth rates:

$$\hat{RQ} = \frac{\frac{\hat{\mu}_o}{Y_{go}} + \frac{\hat{\mu}_r}{Y_{gr}} + \frac{\hat{\mu}_e}{Y_{ge}}}{\frac{\hat{\mu}_o}{Y_{o2}} + \frac{\hat{\mu}_r}{Y_{o2e}}} \tag{13}$$

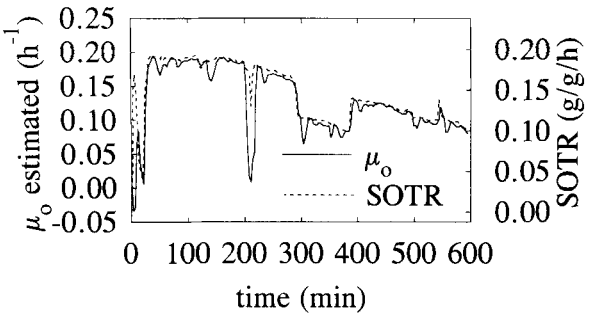

Figure 9. Estimated sugar oxidation specific growth rate and specific oxygen transfer rate in fermentation 1.

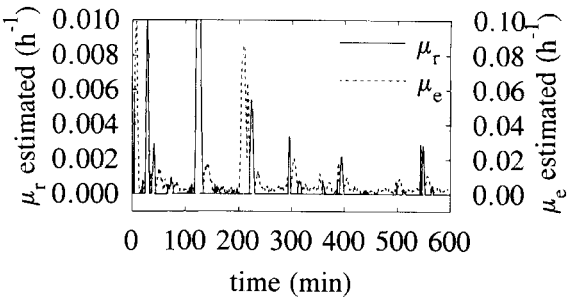

Figure 10. Estimated ethanol oxidation and sugar fermentation specific growth rates in fermentation 1.

The values of each of the three specific growth rate estimates have to be accurate in order to produce a good estimate of the respiratory quotient. Figure 11 shows the comparison between the experimental and the estimated respiratory quotient. A respiratory quotient over 1.06 indicates an ethanol production state and below 1.06 an ethanol consumption state. The agreement between the two curves is very good in spite of the inherent lag of the estimation procedure. This comparison allows us to be confident that the estimation method is coherent.

A second criterion is based on the comparison between the ethanol production/consumption rate evaluated from the filtered derivative of the measured ethanol concentration and the estimated rate derived from the estimated values of the specific growth rates and biomass concentration ($\mu_r * x/Y_{re}$ or $-\mu_e * x/Y_e$). Figure 12 shows this comparison for fermentation 1. The agreement is again very good and this test, based on independent measurement, confirms that the values of the specific growth rate estimates reflect the real process state. Also, this shows that the rapid fluctuations of the estimated specific growth rates are caused by the ability of the process controller to maintain the process at the boundary of ethanol production/consumption states and not by an effect of noise in RQ.

Figures 13, 14 and 15 show the state variables profile for another fermentation (2). This fermentation was less perturbed than the previous one except for the latest part where air flow rate variations occurred. In this fermentation, the efficiency of ethanol regulation kept the process near the boundary between the two states and produced faster transition between them. The agreement between observed and measured biomass

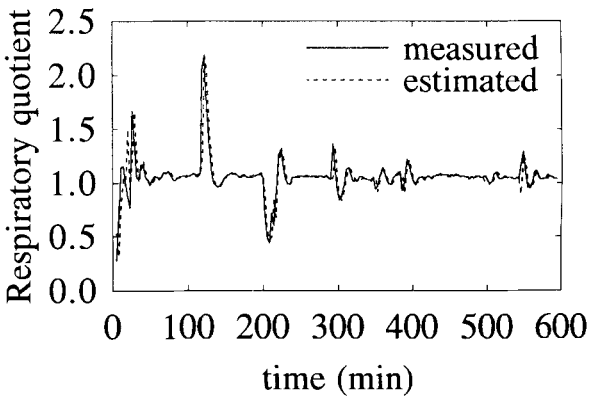

Figure 11. Measured and the estimated respiratory quotient in fermentation 1.

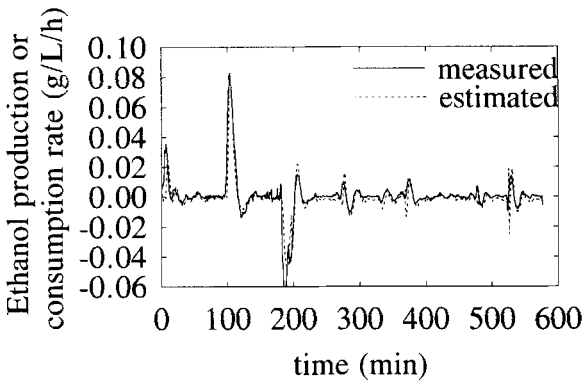

Figure 12. Ethanol production/consumption rate evaluated from ethanol concentration measurement and from specific growth rate estimates in fermentation 1.

concentration (Figure 16) is good except for the last data point. Increased oxygen transfer due to the increased air flow rate is not reflected in the slope of the measured values between the last two samples: the last point might be incorrect. The estimated values of the three specific growth rates, Figures 17 and 18, show the same behavior as in the previous fermentation. The comparison between estimated and evaluated respiratory

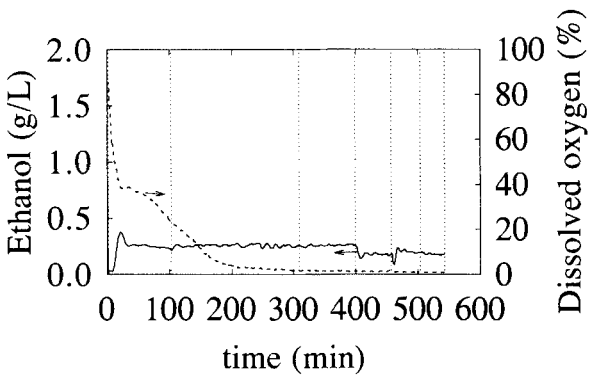

Figure 13. Ethanol and dissolved oxygen concentration in fermentation 2.

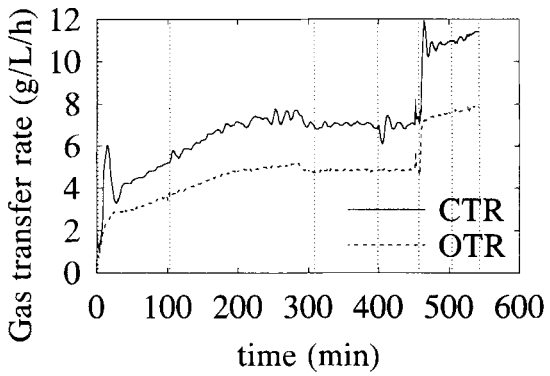

Figure 14. Oxygen and carbon dioxide transfer rate in fermentation 2.

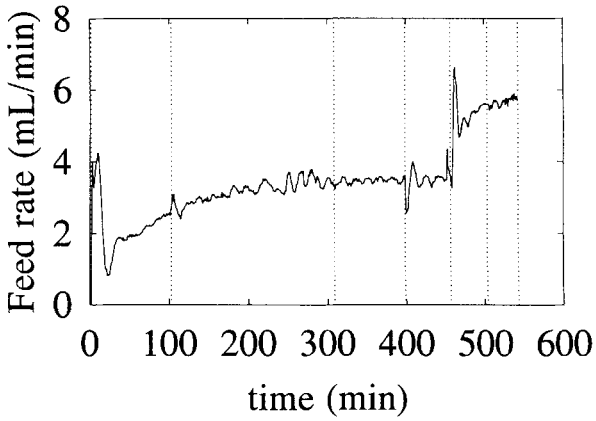

Figure 15. Substrate feed rate in fermentation 2.

quotient shown in Figure 19 indicates that the small fluctuations of the process around the boundary between respiro-fermentative and respirative regions is well reflected in the estimated values of the specific growth rates. The test on ethanol production/consumption rate, Figure 20, demonstrates again the precision of the estimates and that the small variation in RQ values correspond to the real process state and not to measurement noise.

Conclusions

Experimental results obtained from on-line estimation of multiple specific growth rates were presented. Two criteria, based on the respiratory quotient and on ethanol production/consumption rate, were proposed to assess the validity of these results. The accuracy of the estimates depends on the appropriate combination of different factors: the characteristics of the pole placement based estimation algorithm, the alternating use of two sets of algorithms issued from two partial models of the process and the proper selection of the measured state variables set for each partial model. A fast estimation convergence rate, which can be selected by the very simple pole placement parameter, reduces the process and partial model mismatch period at process transition time. The developed transition procedure between the algorithm sets reduces the perturbation caused by the transition. Mathematical and prac-

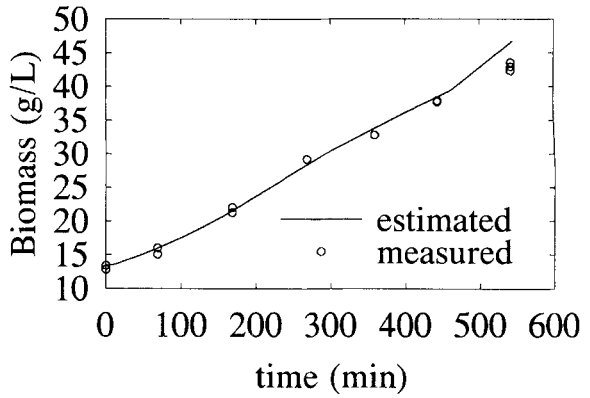

Figure 16. Estimated and measured biomass concentration in fermentation 2.

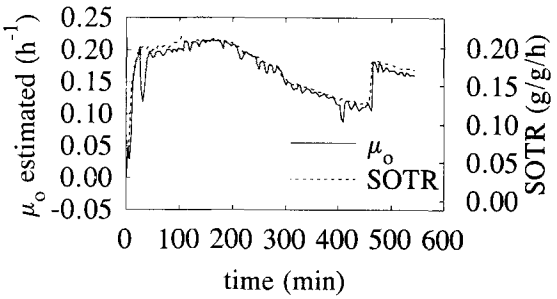

Figure 17. Estimated sugar oxidation specific growth rate and specific oxygen transfer rate in fermentation 2.

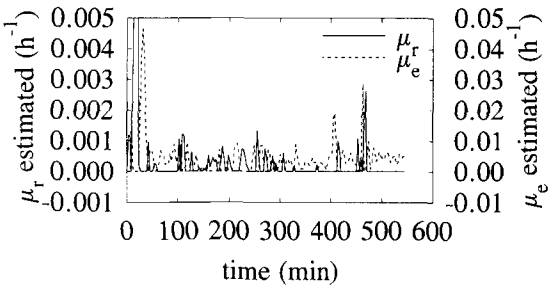

Figure 18. Estimated ethanol oxidation and sugar fermentation specific growth rates in fermentation 2.

tical considerations have been emphasized for the selection of the measured state variables set.

The estimates of the three specific growth rates provide useful information about the process condition. In particular, these results correspond with the yeast limiting respiratory capacity concept in spite of the complete independence of the estimation from any kinetic model or structural concept other than the presence of the three catabolic pathways. The results allow to determine the maximum specific growth rate for sugar oxidation of the yeast strain used, the required decrease in specific growth rate to prevent ethanol formation in limited oxygen transfer condition and the ethanol production or consumption rates in different situations. This information can

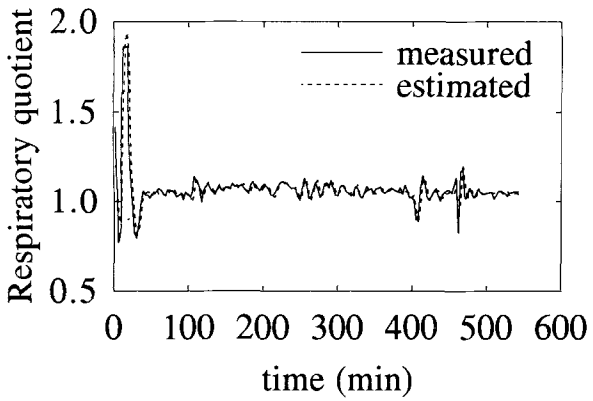

Figure 19. Measured and the estimated respiratory quotient in fermentation 2.

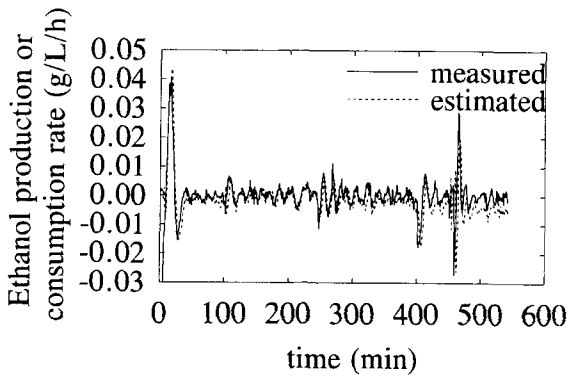

Figure 20. Ethanol production/consumption rate evaluated from ethanol concentration measurement and from specific growth rate estimates in fermentation 1.

be useful to assess the process and equipment performance and also be used in process and plant optimization.

Notation

c = dissolved oxygen concentration
CTR = carbon dioxide transfer rate
D = dilution rate
e = ethanol concentration
g = dissolved carbon dioxide concentration
K = yield coefficient matrix
K_o = unity vector
K_1, K_2 = partition yield coefficient matrices
M = specific maintenance rate vector
M_1,M_2 = partition specific maintenance rate vector
OTR = oxygen transfer rate
p = design parameter: pole in the discrete complex plane
q_{co2man} = carbon dioxide specific maintenance rate
q_{o2man} = oxygen specific maintenance rate
q_{sman} = substrate specific maintenance rate
RQ = respiratory quotient
RQ_o = respiratory quotient associated with sugar oxidation
RQ_f = respiratory quotient associated with sugar fermentation followed by ethanol oxidation
s = substrate concentration
s_i = substrate concentration in the feed
$SOTR$ = oxygen specific transfer rate
t = time
T = sampling period
U = input/output vector
U_1, U_2 = partition input/output vector
x = biomass concentration
Y_i = yield coefficient
Z = transform observer variable

Greek letters

μ_e = specific growth rate associated with ethanol oxidation
μ_0 = specific growth rate associated with sugar oxidation
μ_r = specific growth rate associated with sugar fermentation
ξ = state variable vector
ξ_1, ξ_2 = partition state variable vector
Ψ = transform state variable vector
φ = specific growth rate vector

Subscripts and superscript

t = time
R = respiratory partial model
RF = respiro-fermentative partial model
$\hat{}$ = estimated

Literature Cited

Dochain, D., "On-Line Parameter Estimation, Adaptive State Estimation and Adaptive Control of Fermentation Processes," Doctoral Diss., Université Catholique de Louvain, Belgium (1986).

Dochain, D., and G. Bastin, "Stable Adaptive Algorithms Estimation and Control of Fermentation Processes," Modelling and Control of Biotechnological Processes, Proc. of the First IFAC Symp., A. Johnson (ed), Noordwijkout, Netherlands, Dec. 11-13, 1985, Pergamon Press, 37 (1986).

Nihtila, M., P. Harmo, and M. Perttula, "Real-Time Growth Estimation in Batch Fermentation," *Bridge Between Control Science and Technology, Proc. Triennial World Cong. of IFAC*, Budapest, Hungary, **4**, 1825 (1984).

Narendra, K. S., and A. M. Annaswany, *Stable Adaptive System*, Prentice Hall Information and System Sciences Series, Englewood Cliffs, NJ (1989).

Pomerleau, Y., "Modélisation et Controle d'un Procédé Fed-Batch de Culture des Levures à Pain (Saccharomyces cerevisiae)," PhD Thesis, Ecole Polytechnique de Montréal (1990).

Pomerleau, Y., and M. Perrier, "Estimation of Multiple Specific Growth Rates in Bioprocesses," *AIChE J.*, **36**(2), 207 (1990).

Sastry, S., and M. Bodson, *Adaptive Control, Stability, Convergence, and Robustness*, Prentice Hall, Englewood Cliffs, NJ (1989).

Sonnleitner, B., and O. Kappeli, "Growth of Saccharomyces cerevisiae is Controlled by its Limited Respiratory Capacity: Formulation and Verification of a Hypothesis," *Biotech. Bioeng.*, **28**, 927 (1986).

Stephanopoulos, G., and K. Y. San, "Studies on On-Line Bioreactor Identification: I. Theory," *Biotech. Bioeng.*, **26**, 1176 (1984).

Manuscript received Oct. 15, 1991, and revision received Jun. 8, 1992.